

# Bone Marrow Derived Mesenchymal Stem Cells Versus Astaxanthin in Treatment of Toxic Effect of 5-Fluorouracil on Gastric mucosa of Male Albino Rats

Amal M. ElSafy Elshazly<sup>1</sup>, Neama Mahmoud Taha <sup>2</sup>, Naglaa

A.S. Sarg<sup>1</sup>, Asmaa Y.A. Hussein <sup>3</sup>, Yasmeen Mohammed Ismail El Sayed <sup>4</sup>, Haidy M.Fakher<sup>3</sup>, and Ali Mohamed Ali <sup>1</sup>.

Department of Anatomy and Embryology Faculty of Medicine, Benha University <sup>1</sup>.

Physiology Department, Umm Al-Qura University, KSA <sup>2</sup>.

Department of Forensic Medicine and Clinical Toxicology Faculty of Medicine, Benha University <sup>3</sup>.

Department of pharmacology Faculty of Medicine, Benha University<sup>4</sup>.

Corresponding author: Amal Elshazly,

Mobile:(+20)1222924128,Email:[amal.elshazly79@yahoo.com](mailto:amal.elshazly79@yahoo.com)

<https://orcid.org/0000-00031051-7241>

**Abstract:** 5-fluorouracil (5-FU) is an effective chemotherapeutic medication. It is commonly implicated in treatment of various malignancies; this research aimed to investigate potential therapeutic effect of the BMMSCs and Astaxanthin on 5-FU toxic effect on albino rat's stomach. 40 rats were divided into 4 groups: Group I (control group): received no treatment Group II (5-fluorouracil group): for 5 consecutive days rats were intravenously injected by 50 mg/kg 5-FU. Group III (5-Fluorouracil group and Astaxanthin): got 5-FU as in group II, followed by astaxanthin 50mg/kg for 10 consecutive days. Group IV (BMMSCs): received 5-FU as in group II then intravenously injected by 10<sup>6</sup> of BMMSCs once in rat tail. All rats were sacrificed on the 35<sup>th</sup> day from the beginning of the experiment, to be examined microscopically, stomach sections were stained by H&E to evaluate histopathological changes, stained also with PAS to evaluate mucosal glycoprotein production, transmission electron microscopic was used to evaluate ultra-structural changes and Immunohistochemistry using Ki67 was used to evaluate level of cell proliferation. examination of stomach Sections of group II showed separation in the gastric glands, congested blood capillary, vacuolations of parietal cells, while (Gr III) and (Gr IV) showed marked stomach histological structure improvement and down regulated expression of Ki67, compared to the (GrII). electron microscope supported these results. Both BMMSCs and Astaxanthin have good impact in ameliorating the toxic effect of 5-FU on albino rats stomach, with no significant difference between both techniques.

**Key words:** Astaxanthin,5FU,stomach,MSCs.

## Introduction:

Chemotherapy includes the use of cytotoxic agents to eradicate neoplastic cancer cells in different organs (Ferlay et al., 2015). 5-fluorouracil (5-FU) is an effective antimetabolite chemotherapeutic medication. It is commonly implicated in various malignancies treatment as colorectal, liver, head, neck skin, and breast cancers (Bachmeier et al., 2019). Regarding the National Comprehensive Cancer Network and the European Society for Medical Oncology guidelines, 5-FU is a crucial medicine for

both adjuvant therapy and metastatic colorectal cancer (Benson et al., 2017). 5FU is activated by thymidine phosphorlylase enzyme into fluoro - deoxyuridylate which is capable of suppressing thymidylate synthetase, resulting in direct inhibition of DNA synthesis. (Kataoka et al., 2010)

There is a consistent and long history of 5-FU in mucosal injury induction. It causes lesions in the form of inflammation and ulceration at any region of the gastrointestinal system, causing a variety of symptoms that significantly influence the tolerance of chemotherapy and quality of life is the definition of mucositis (Gawish et al., 2013).

Astaxanthin is a carotenoid pigment with a powerful antioxidative and anti-inflammatory effects. It is the most potent and safest antioxidant known to exist in nature. Numerous types of algae, plants, and types of seafood, such as shrimp and salmon fish, are typical natural sources of Astaxanthin. It is derived from *Haematococcus pluvialis* microalgae (Mosaad et al., 2016).

Astaxanthin, has been found to be highly effective in mopping up free radicals as it possesses anti-oxidative, anti-inflammatory, anti-apoptotic, and other beneficial pharmacological properties. Many chemical reactions produce free radicals which are injurious to body cells, as they are the causes of many diseases, disabilities, and death. Antioxidants suppress and mop up these circulating free radicals (Kim et al., 2018).

Stem cell therapy refers to any technique that uses or stimulates stem cells. Typically, it serves to repair or replace damaged cells or tissues (Rashed et al., 2016). Bone marrow-mesenchymal stem cells (BMMSCs) were reported by multiple studies to had a valuable role in the gut damage healing and contribute to the gastrointestinal tissue's development (Liu et al., 2015).

Askarov et al., (2008) found that multipotent mesenchymal stromal cells derived from autologous bone marrow may promote gastric mucosa microcirculation, stimulate angiogenesis, and enhance gastric ulcer healing in rats

This study aimed to assess 5-FU effect on gastric mucosa and compare between the beneficial regenerative effects of BMMSCs and Astaxanthin on 5-FU- induced gastric toxic lesions.

## **Materials and Methods**

### **Experimental animals:**

This study was carried out on Forty healthy adult male albino rats with an average weight of 250 gm for each rat from the animal house, Faculty of Veterinary Medicine, Benha University, Egypt. Rats were kept under conventional conditions of temperature (22 + 2C), 12-h light/12-h dark cycles, relative humidity (45–65%), they had unrestricted access to a conventional pellet diet and purified water. Rats were put under perfect sanitary conditions.

### **BM- MSCs preparation:**

With a DMEM (GIBCO / BRL) solution containing 10% fetal bovine medium (GIBCO/BRL) , bone marrow was collected by flushing tibiae and femurs of male rats

aged 6 weeks. Using a density gradient [Ficoll/ Paque (Pharmacia)] , nucleated cells have been then resuspended in 1 % penicillin-streptomycin (GIBCO/BRL) culture media. Either as a primary culture or after big colonies had grown, the cells were kept in a CO<sub>2</sub> incubator at 5% CO<sub>2</sub> humidity and 37 °C for 12-14 days. When the cultures achieved 80-90% confluence after being washed twice with PBS, at 37 °C for 5 minutes they were trypsinized with 0.25 % trypsin in 1ml EDTA (GIBCO/BRL). PBS was used to resuspend the cells after centrifugation. Identifying MSCs in culture involves looking for adhesion, a fusiform morphology, and the RTPCR detection of the surface marker CD29. (Bruno et al., 2012).

**Labeling Of Stem Cells with PKH26 Dye:** The MSCs were isolated and fluorescently labelled with PKH26 linker dye during the 4<sup>th</sup> passage. Excitation of PKH26 (a red fluorochrome) occurs at 551 nm and emission at 567 nm. In the labeled cells, both proliferative and biological activity is preserved. The linker is thus suitable for long-term in vivo cell tracking, in vitro cell labeling, and in vitro cell proliferation research. The dye is stable and will divide proportionally when the cells divide. Detection of injected cells homing in the rat's stomach: At the end of the experiment, the stomach of the rat was examined using a fluorescence microscope to identify the PKH26-stained cells, demonstrating that the injected cells had engrafted into (Gr IV) stomachs (Alexandra et al., 2017).

**Drugs:**

1. 5-FU manufactured by Pharco Egypt (Cairo, Egypt) 250 mg/5 ml ampoules.
2. Astaxanthin was purchased online by Biovea Egypt. It is manufactured by (Solabia -Algatech nutrition) in the form of soft gel capsules each one contains 42mg of Astapure oil providing 4 mg of Astaxanthin.
3. BMMSCs: From the stem cell research unit at Faculty of Medicine, Banha University, Histology Department, BMMSCs extract was obtained.

**Experimental design:**

Rats were separated into 4 distinct groups.

:

**Group I (control group):** receive no treatment..

**Group II (5-fluorouracil group):** intravenously injected in the tail vein with 50 mg/kg 5-FU for 5 consecutive days . (El-Bermawy, 2015).

**Group III (5-fluorouracil group and Astaxanthin):** received 5-FU as in group (II) for 5 consecutive days, then they received 50 mg/kg Astaxanthin (Gorkem et al., 2018). For 10 consecutive days, each rat received the oily content of three soft gel capsules once daily by nasogastric tube .

**Group IV (5-fluorouracil group and BMSCs):** received 5-FU as in group (II) for 5 consecutive days then intravenously injected in the tail vein with  $10^6$  cells of BMSCs. (Rashed et al., 2018).

All rats were sacrificed on the 35<sup>th</sup> day from the beginning of the experiment

#### **Tissue collection and preparation**

Rats were sacrificed by cervical dislocation after being anesthetized by receiving an overdose of anesthesia ( $\geq 0.86$  mg/kg sodium pentobarbital intraperitoneally). To eliminate blood clots, stomachs were opened along the greater curvature after their collection from animals, and flushed in cooled phosphate buffered saline (PBS). Each stomach tissue was separated equally into right and left halves. All animals' left halves were immediately submerged in 10% formalin for immunohistochemical and histopathological assessment.

#### **Histopathological studies:**

Section obtained from albino rat stomach transformed into paraffin blocks. These blocks were sectioned using a rotary microtome to a thickness of 5  $\mu$ m. (LEICA RM 2125; UK). Hematoxylin & Eosin (H&E), a standard histological stain used to analyze any histological changes, then to assess mucosal glycoprotein production were stained with PAS and for microscopic examination of any regenerative process and gastric injury they were stained by H&E. (Kim et al., 2019).

#### **Immunohistochemical studies:**

The sections were immunostained using avidin-biotin technique. The sections were stained with rabbit anti-Ki-67 antiserum (Sigma- Aldrich, St Louis, USA) (Takkem et al., 2018).

**Morphometric study:** The image analysis software program (Image j. 1.46version) was used to examine sections from the fundal mucosa in all groups. The optical density of PAS stain was measured in 5 randomly different microscopic fields in each specimen at x400 magnification power.

The Ki67-immuno-expression mean area percentage was calculated using 5 images from 5 non-overlapping fields.

#### **Electron microscopic studies:**

A Transmission electron microscopy (TEM) was used to analyse 1 mm<sup>3</sup> stomach specimens which were fixed with 2.5 % glutaraldehyde in 0.1 M PBS (pH 7.4) for 2 hrs. at 4 °C, followed by 1.5 hours of post-fixation with 1 % osmium tetroxide at the same temperature. The samples were immersed in a series of ethanol dilutions (50, 70, 90, 95, and 4-times 100 %, each for 15 minutes) and then dehydrated in acetone for 30 min. The specimens were finally implanted with epoxy resin (Epoxy Embedding Medium Kit; Sigma). Using an ultramicrotome (RMC PT-XL Power Tome Ultramicrotome), Sections were cut at varying thicknesses as semi- and ultra-thin sections. Using an Olympus BX61 light microscope, the semithin (1  $\mu$ m) slices were stained with 1% toluidine blue and inspected. 70 to 90 nm thick ultrathin slices were cut and stained with 2.5 % uranyl acetate as a primary stain and lead citrate as the counter stain. (Bancroft et al., 2018). At the electron microscope unit of the faculty of

medicine at Benha University in Egypt, the ultrathin sections were subsequently analyzed with a JEM-1400 Plus TEM (JEOL, Japan).

### **Ethical approval:**

This experimental research was reviewed and approved in accordance to the Faculty of Medicine, Benha University Research Ethical Committee Recommendations, Rc.13.10.2022

### **Statistical analysis**

IBM's SPSS Statistics for Windows, Version 19, (IBM Corp., Armonk, NY, USA) was used to collect and analyse the experiment's data. One-way analysis of variance and a Post Hoc LSD test were used to analyse the data and find significant differences between the groups. Each test's findings were reported using a mean and standard deviation, and a two tailed P value < 0.05 was considered statistically significant.

### **Results**

The histopathological result revealed long, straight, densely packed gastric glands bordered with normal surface columnar cells with basal oval nuclei were seen in the fundic mucosa of the control group's stomachs, normal mucous neck cells with basal flattened nuclei and normal apical surface columnar epithelium and light foamy cytoplasm. Parietal cells appeared large polyhedral with acidophilic cytoplasm with central rounded nuclei , prominent nucleoli and chief cells with basal nuclei (Figure 1).

Stomach sections from fundal mucosa of group II showed desquamation of surface epithelial cells into the lumen, separation in the gastric glands, massive dilated congested blood capillary and vacuolations of parietal cells with pyknotic nuclei. Distorted chief cells with pyknotic nuclei could be observed. Massive mononuclear cellular infiltration was noticed in the lamina propria and in between fundal glands (Figures 2A&2B). Deep ulceration reaching the muscularis mucosa was also noted . (Figure 2C)

Stomach section in the fundic mucosa of group III showed desquamation areas in surface columnar epithelium, mild infiltration with inflammatory cells in between gastric glands and nearly normal some parietal cells and others with pale vacuolated cytoplasm (Figure 3).

Stomach sections from fundal mucosa of group IV showed more or less normal apical surface columnar epithelium and mucous neck cells with flat basal nuclei. Parietal cells appeared rounded with acidophilic cytoplasm and central vesicular nuclei few parietal cells showed vacuolated cytoplasm (Figure 4).

While Periodic Acid Schiff (PAS) stained sections in fundal gastric mucosa of control group stained with Periodic Acid Schiff (PAS) showed intense (PAS) stain positivity of the surface epithelium. (Figure 5A)

The mucous layer in group II showed that fundal mucosa was completely depleted, as revealed by the absence of PAS staining. (Figure 5B)

In the PAS-stained fundal gastric mucosa of group III, there was a moderate growth of a large, continuous PAS positive mucous gel layer that covered the whole stomach mucosal surface (Figure 5C)

Fundal gastric mucosa stained by PAS of group IV (MSC) showed positive PAS stain as bright color to the mucous cells of the surface epithelium and lining the gastric pits. (Figure 5D)

About Ki67 stained sections, ki67 immunostained fundal gastric mucosa of control group showed negative Ki67 immunoreaction. limited number of cells were proliferated, and no lymphocytic aggregation can be seen (Figure 6A).

ki67 immunostained fundal gastric mucosa of group II showing strong positive Ki67 immunoreaction can be detected in many nuclei of proliferative cells lining the isthmus, neck of the gastric glands (Figure 6B)

ki67 immunostained fundal gastric mucosa of group III showed moderate positive Ki67 immunoreaction in the nuclei of cells lining the isthmus of gastric glands (Figure 6C).

ki67 immunostained fundal gastric mucosa of group IV showed mild positive Ki67 immunoreaction was observed in little number of proliferative cells lining the isthmus (Figure 6D).

PKH26 fluorescent -stained sections of the fundal gastric mucosa in BMSC group revealed a numerous red fluorescent cells dispersed throughout the entire fundal gastric mucosa. (Figure 7).

In transmission electron microscopic result, the ultrastructure examination of mucus surface cells of the control group appeared with regular and oval nucleus with prominent nucleolus and surrounded by normal RER and normal mitochondria. Cells had apical microvilli and apical mucinogen granules (Figure 8A)

Electron micrograph of parietal cells of the fundal gastric mucosa of the control group revealed, large pyramidal cells having; intracellular canaliculi, smooth endoplasmic reticulum (SER), numerous mitochondria and central spherical nuclei with prominent nucleoli. Enteroendocrine cells showed regular rounded nuclei surrounded by normal (RER), homogeneous cytoplasm and secretory granules (Figure 8B&8C).

The ultrastructure examination of surface columnar cells of group II revealed loss of junctional complex between columnar cells and sparse apical microvilli, mild to massive depletion of secretory mucinogen granules and the nuclei appeared indented while some of them were distorted and the nuclei appeared irregular (Figure 9A&9B).

The ultrastructure examination of the fundal gastric mucosa, parietal cells of group II showed dilated SER, few cytoplasmic vacuoles, normal mitochondria, pyknotic

shrunken nuclei, eosinophilic infiltration between parietal cell was observed (Figures 9C,9D&9E).

Enteroendocrine cells of group II showed indented nuclei surrounded by dilated perinuclear membrane, vacuolated cytoplasm, secretory granules and nearly normal golgi apparatus was observed (Figure 9F).

The ultrastructure examination of surface columnar cells of group III revealed indented nuclei surrounded by homogeneous cytoplasm, mitochondria, RER, apical mucinogen granules (Figure 10A): Parietal cells of the fundic gastric mucosa of the group showed, large pyramidal cells with regular normal spherical nuclei surrounded by large number of normal mitochondria. Mild damaged in intracellular canaliculi could be seen (Figure 10B) Enteroendocrine cell of the group III showing irregular indented nucleus, surrounded by normal RER, homogenous cytoplasm, secretory granules and dilated golgi (can be observed. (Figure 10C).

The ultrastructure examinations of surface columnar cells of group IV appeared tall columnar cells having apical microvilli, apical mucinogen granules and basal oval nuclei with prominent nucleoli (Figure 11A). Parietal cells of the gastric mucosa of group IV revealed regular normal spherical nuclei surrounded by large number of mitochondria (Figure 11B).

Enteroendocrine cells showed regular rounded nuclei surrounded by normal RER, homogeneous cytoplasm. Mild depletion of secretory granules could be detected (Figure 11C).

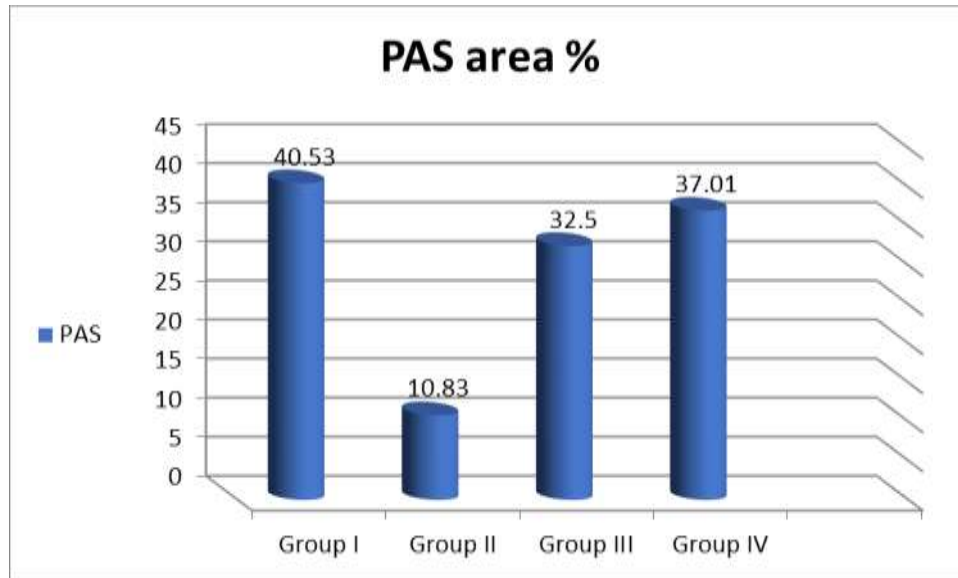
About the morphometric results, table (1) and histogram (I) showed the PAS stain mean area percent in stomach sections across all groups, and table (2) and histogram (I) showed Ki67 expression mean area percent in stomach sections across all groups. The mean area percent of Ki67-immunopositive expression in the stomach sections was significantly increased in GII compared to GI. The mean area percent of Ki67-immunopositive expression in the stomach sections was significantly reduced in G III and GIV compared to G II. But G IV showed no statistically significant difference in Ki67 immuno-positive expression mean area percent compared to G III. While PAS-stain mean area percent of stomach sections was significantly decreased in GII compared to GI. And the mean area percent of PAS stain in the stomach sections was significantly increased in G III and GIV compared to G II. But G IV showed no statistically significant difference in PAS stain mean area percent compared to G III.

**Table (1) showing mean values of area percent PAS ± SD in the 4 groups. (Total number of sections=40 , five sections in each group )**

Mean%± SD	Group I	Group II	Group III	Group IV
PAS %	40.53 ± 4.4	10.83 ± 2.3	32.5 ± 1.4	37.01 ± 2.3

<b>P- value</b>	I versus II = 0.000 I versus III = 0.034 I versus IV = 0.467	II versus I = 0.000 II versus III = 0.000 II versus IV = 0.000	III versus I = 0.034 III versus II = 0.000 III versus IV = 0.280	IV versus I = 0.467 IV versus II = 0.000 IV versus III = 0.280
<b>Significance ≤ 0.05</b>	With groups II & III	With groups I, III & IV	With groups I & II	With group II

The data are shown as the mean ± standard deviation SD (in each group).



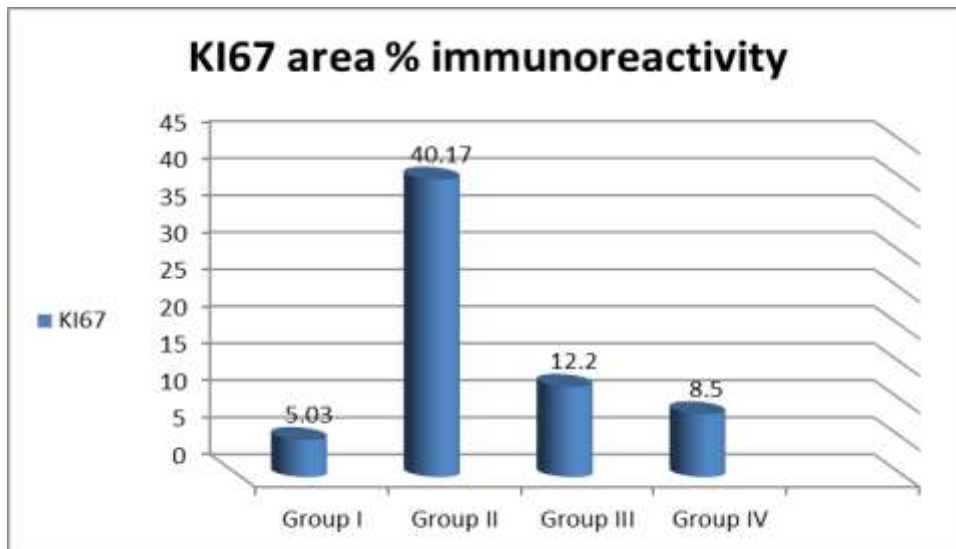
**Histogram (I) showing mean values of area percent of PAS in the 4 groups.**

**Table (2) showing mean values of area percent KI67 immunoreactivity ± SD in the 4 groups. (Total number of sections = 40, five sections in each group)**

Mean % ± SD	Group I	Group II	Group III	Group IV
<b>KI67 %</b>	5.03 ± 1.4	40.17 ± 10.5	12.2 ± 0.95	8.5 ± 1.1
<b>P- value</b>	I versus II = 0.000 I versus III = 0.414 I versus IV = 0.857	II versus I = 0.000 II versus III = 0.01 II versus IV = 0.000	III versus I = 0.414 III versus II = 0.001 III versus IV = 0.833	IV versus I = 0.857 IV versus II = 0.000 IV versus III = 0.833
<b>Significance ≤ 0.05</b>	With group II	With groups I, III & IV	With group II	With group II

The data are shown as the mean ± standard deviation SD (in each group)





**Histogram (II) showing mean values of area percent of KI67 Immunoreactivity in the four groups.**

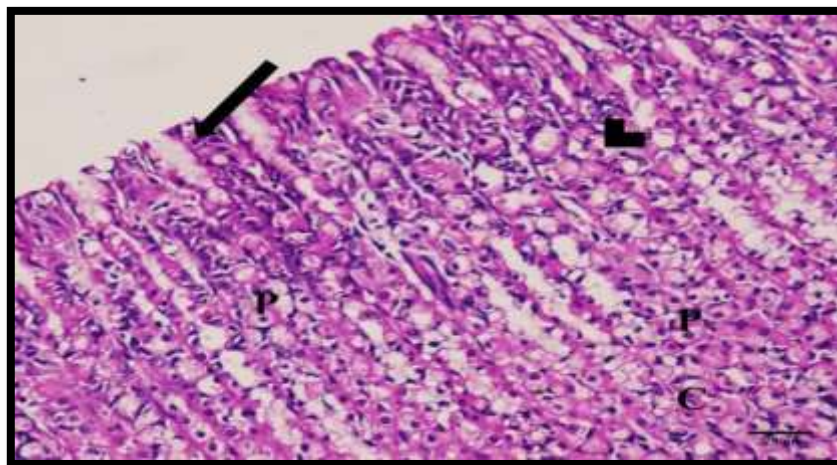


**Fig.(1):** A photomicrograph of a section in rat stomach fundal mucosa of control group revealed apical surface columnar epithelium (arrow), mucous neck cells (arrowhead) with flat basal nuclei & pale foamy cytoplasm. Parietal cells (P) appeared large polyhedral with acidophilic cytoplasm & central rounded nuclei and prominent nucleolus. Chief cells (C) with basal nuclei. (H&E  $\times$ 400).

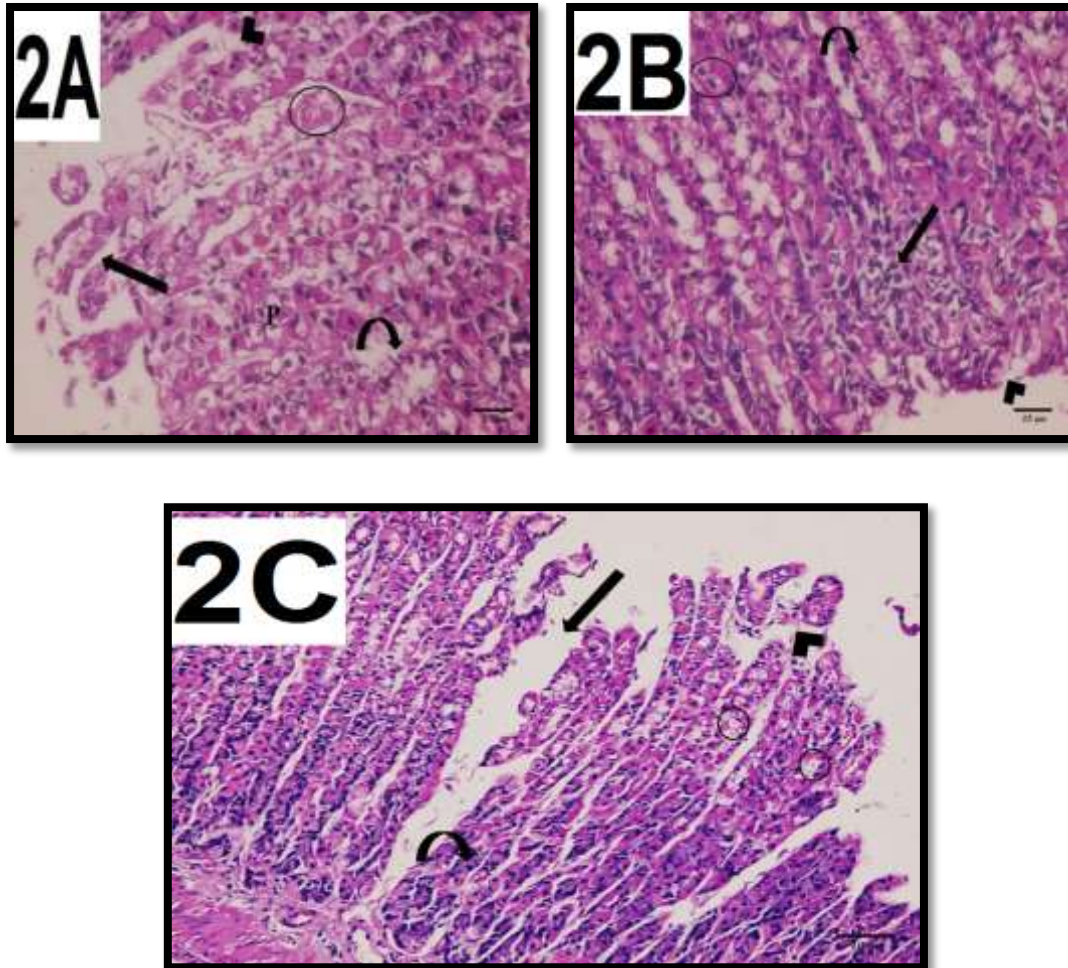


**Fig. (2):** A photomicrograph of a stomach section in the fundal mucosa of group II: (2A) showed desquamation of surface epithelial cells into the lumen (arrow), separation in the gastric glands (arrowhead), massive dilated congested blood capillary (circle), vacuolations of parietal cells with eccentric pyknotic nuclei (P), mucous neck cells with basal pyknotic nuclei (curved arrow). (H&E  $\times 400$ ), (2B) showing massive mononuclear cellular infiltration (arrow) is noticed in between fundal glands, widening of gastric pits (arrowhead) can be observed. Ballooned parietal cells with vacuolated cytoplasm (circle), mucous neck cells with basal pyknotic nuclei (curved arrow). (H&E  $\times 400$ ), and (2C) showing deep ulceration (arrow) reaching the muscularis mucosa, exfoliation and desquamation of the superficial gastric epithelium (arrowhead) and separation between fundal glands, some parietal cells appeared with vacuolated cytoplasm (circle), distorted chief cells with pyknotic nuclei (curved arrow). (H&E  $\times 200$ ).

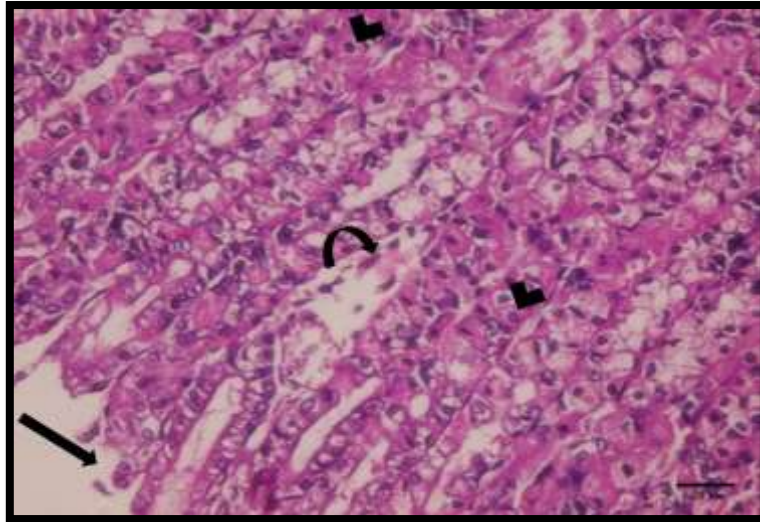


**Fig. (3):** A photomicrograph of a stomach section in the fundal mucosa of group III showed desquamation in surface columnar epithelium (arrow), mild infiltration with inflammatory cells in between gastric glands (curved arrow), nearly normal parietal cells (arrowhead) and other showing vacuolated cytoplasm (H&E  $\times 400$ )

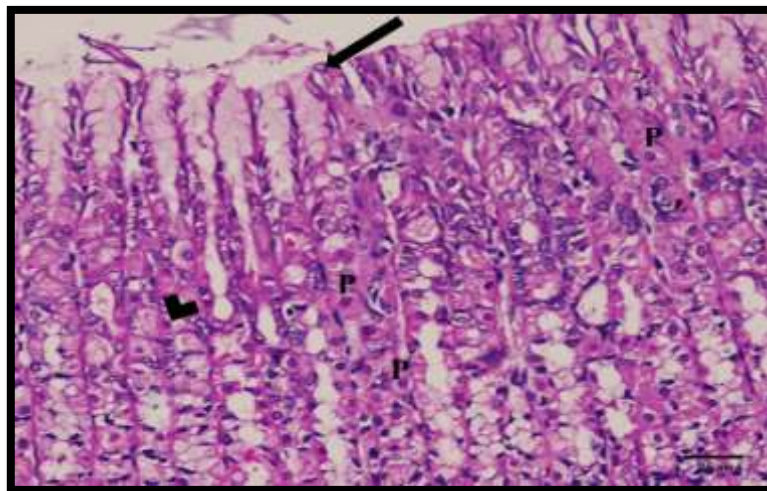


**Fig. (4):** A photomicrograph of a stomach section in the fundic mucosa of group IV showed more or less normal apical surface columnar epithelium (arrow), mucous neck cells (arrowhead) with flat basal nuclei. Parietal cells (P) appeared rounded with acidophilic cytoplasm & central vesicular nuclei; notice few parietal cells showing vacuolated cytoplasm. (H&E  $\times 400$ ).



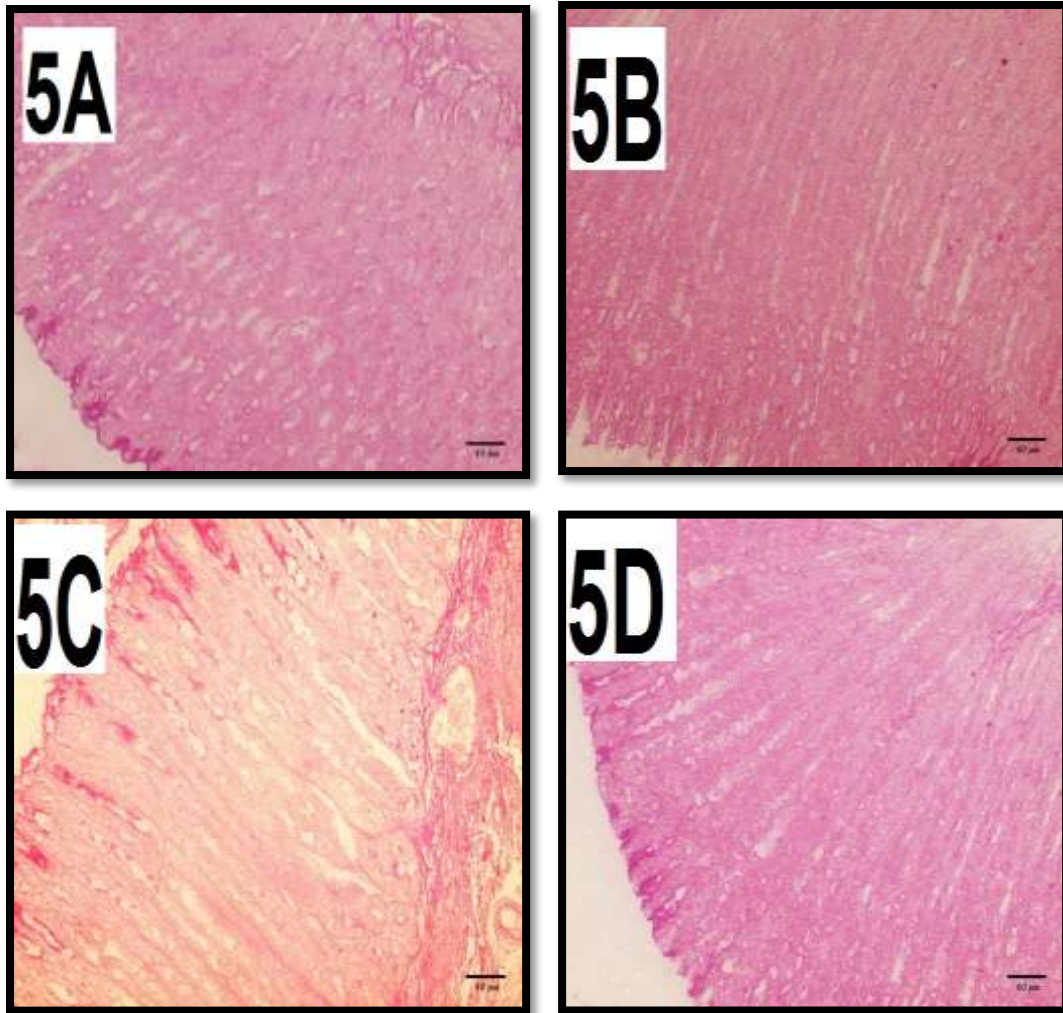


**Fig. (5):** A Photomicrograph of PAS stained fundic gastric mucosa: (5A) sections from control group showing intense PAS positivity of the surface epithelium, (5B) sections from group II showed complete depletion to the mucous layer as seen by the absence of PAS stain, (5C) group III sections demonstrate moderate expansion of substantial continuous PAS positive mucous gel layer that covering the entire gastric mucosal surface. And (5D) sections from of group IV (MSC) showing positive PAS stain as bright colour to the mucous cells of the surface epithelium and lining the gastric pits. (5A,5B,5C, ana5D all are PAS x200).

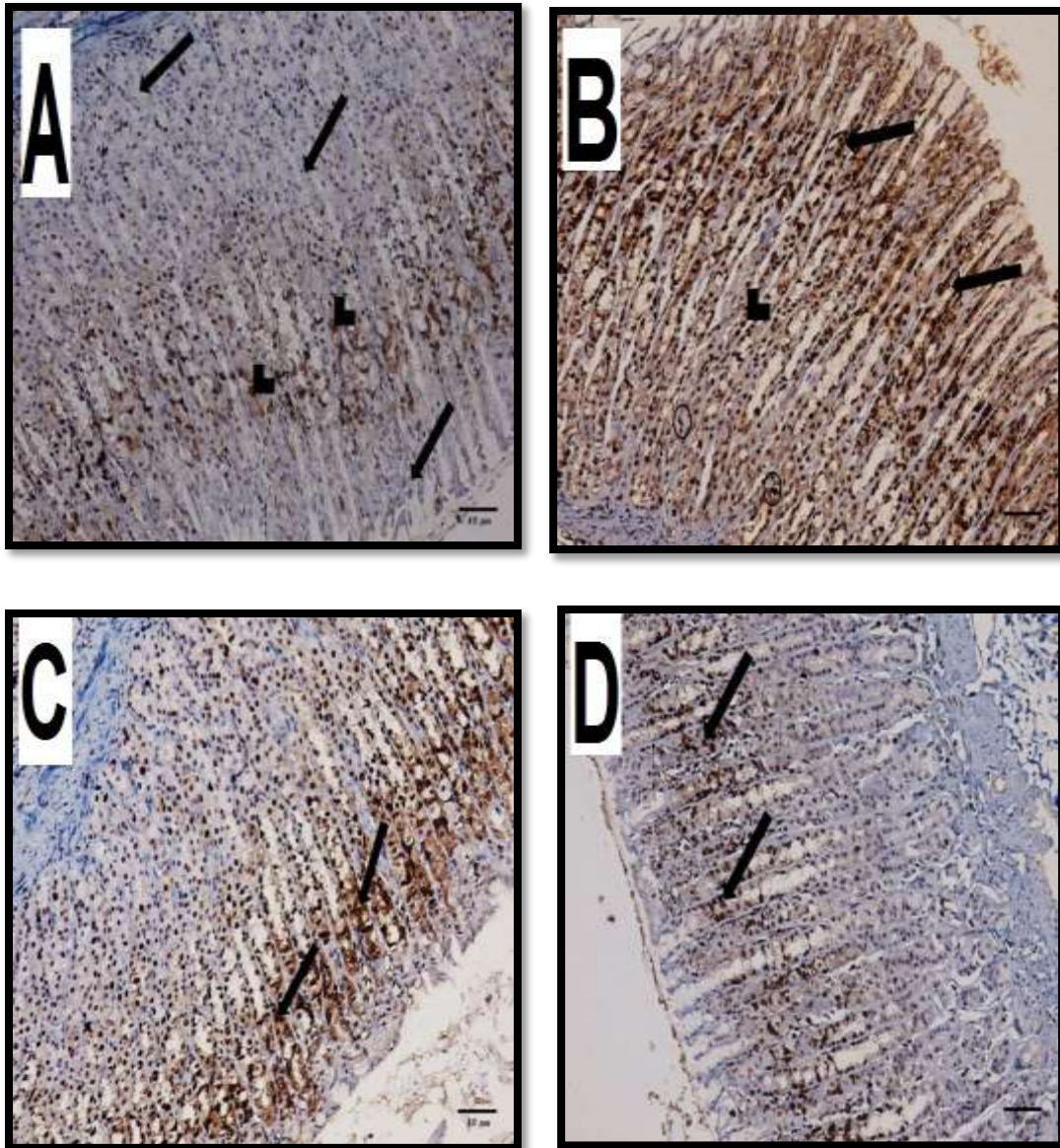


**Fig. (6):**A Photomicrograph of ki67 immunostained fundic gastric mucosa: (A) sections of control group showed negative Ki67 immunoreaction was observed in most of the fundal glands cells (arrow),there are limited number of cells are proliferating (arrow head) and no lymphocytic aggregates can be seen, (B) section of group II showed strong positive Ki67 immunoreaction can be detected in many nuclei of proliferative cells lining the isthmus (arrow), neck of the gastric glands (arrow head) and base (circle) ,(C)section of group III showed moderate positive Ki67 immunoreaction was observed in the nuclei of cells lining the isthmus of gastric glands (arrow) ,and (D) section of group IV showed mild positive Ki67 immunoreaction was observed in little number of proliferative cells lining the isthmus (arrow) (A,B,C and D all Ki67 x200).

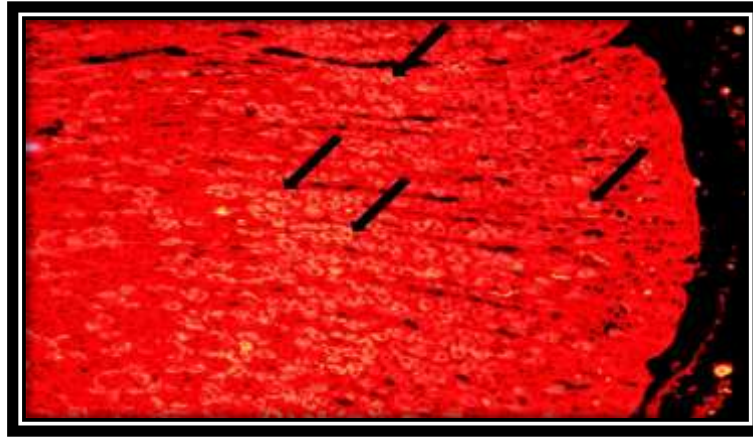


**Fig. (7):** A Photomicrographs of PKH26 fluorescent-stained sections revealed many red fluorescent cells distributed all over the fundal gastric mucosa in BMSC group (PKH26  $\times 200$ )



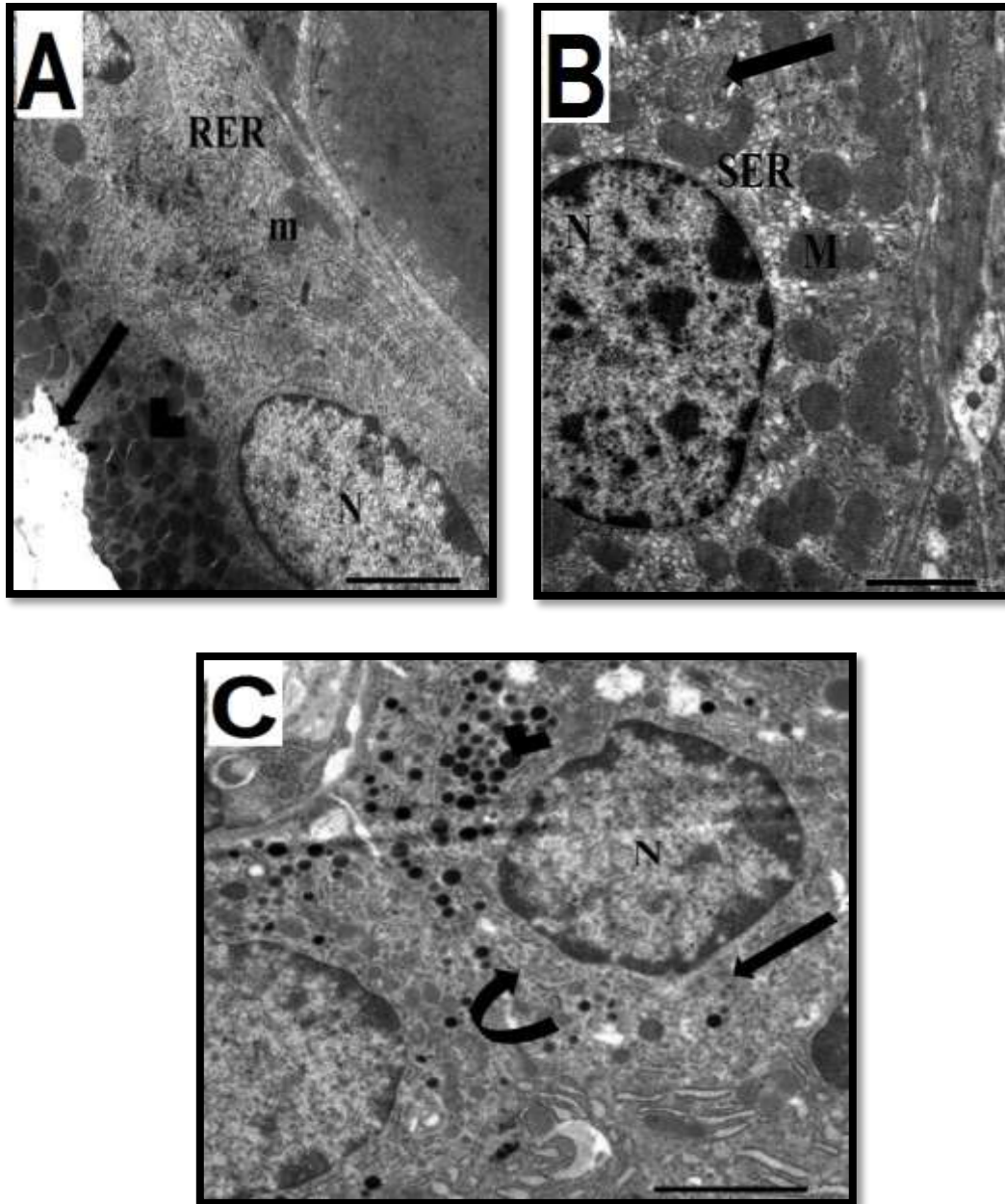


**Fig. (8):** (A) An electron micrograph of mucus surface cell of the control group appeared with regular and oval nucleus (N) with prominent nucleolus surrounded by normal RER, mitochondria (m), cell having apical microvilli (arrow), apical mucinogen granules (arrowhead). (TEM X 20000)

(B) An electron micrograph of parietal cell of the fundic gastric mucosa of the control group showed, large pyramidal cell having; intracellular canaliculi (arrow), smooth endoplasmic reticulum SER, numerous mitochondria (M) and central spherical nucleus (N) with prominent nucleolus. (TEM X 20000)

(C) An electron micrograph of enteroendocrine cell of the control group showed regular rounded nucleus (N) surrounded by normal RER, homogenous cytoplasm (arrow), secretory granules (arrowhead). (TEM X 20000)

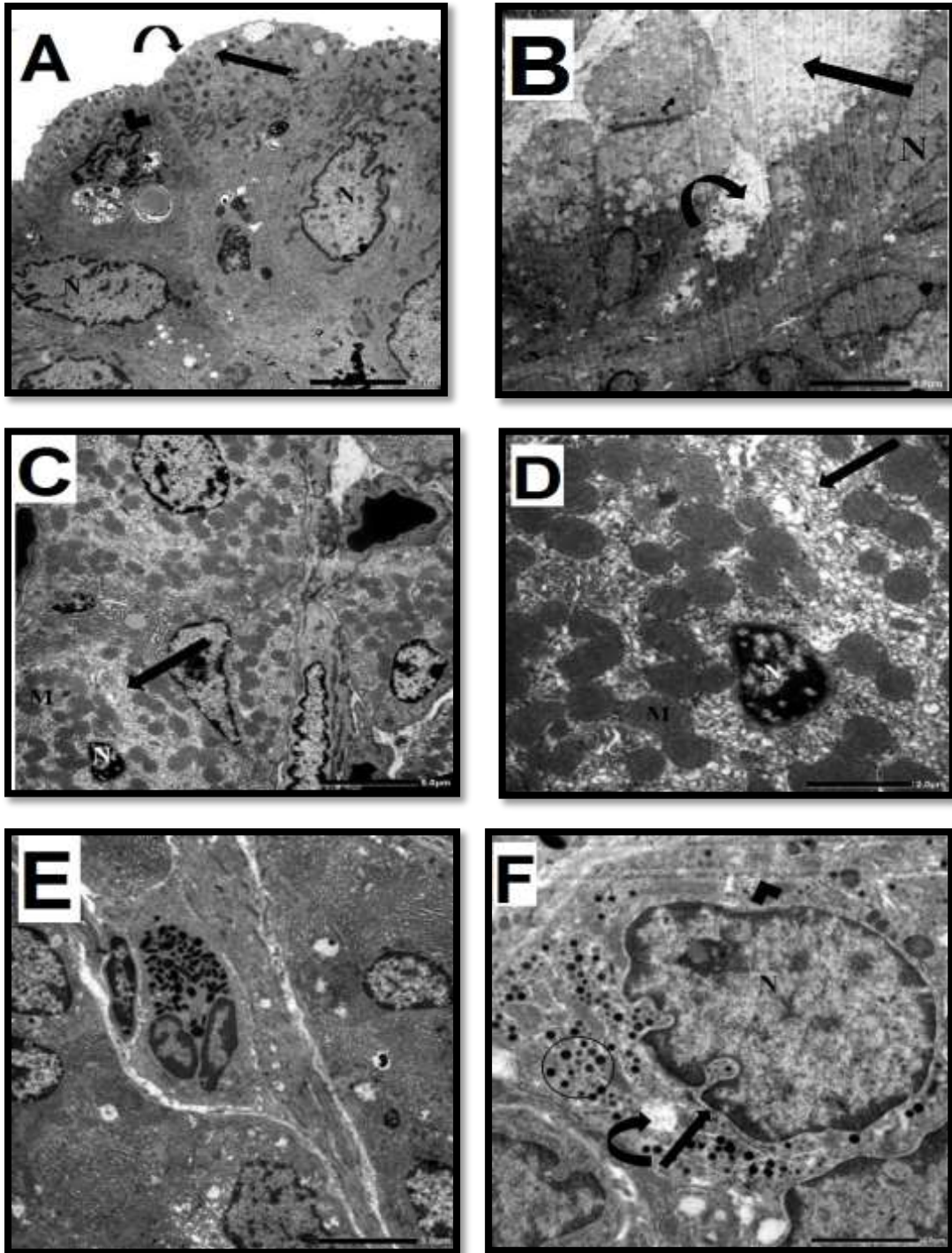


Fig. (9) (A): An electron micrograph of surface columnar cell of group II showed sparse apical microvilli (curved arrow), mild depletion of secretory mucinogen granules (arrow), and the nucleus appeared indented (N) while one of them was distorted (arrowhead).

(B): An electron micrograph of surface columnar cell of group II showed loss of junctional complex between columnar cell (curved arrow), massive depletion of secretory mucinogen granules (arrow), and the nucleus appeared irregular (N).



**(C):** An electron micrograph of parietal cell of the fundal gastric mucosa from group II showed dilated SER (arrow), few cytoplasmic vacuoles, normal mitochondria (M), pyknotic shrunken nucleus (N). (A, B and D all are TEM X 7000)

**(D):** Is a higher magnification of the previous image, An electron micrograph of parietal cell of the fundal gastric mucosa from group II showed dilated SER (arrow), few cytoplasmic vacuoles, normal mitochondria (M), pyknotic shrunken nucleus (N). (TEM X20000)

**(E):** An electron micrograph of parietal cell of the fundal gastric mucosa from group II showed eosinophilic infiltration between parietal cell (arrow). (TEM X7000)

**(F):** An electron micrograph of enteroendocrine cell of the group II showed indented nucleus (N) surrounded by dilated perinuclear membrane (arrow), vacuolated cytoplasm (curved arrow), secretory granules circle). (TEM X 20000)

Note nearly normal golgi apparatus can be observed (arrowhead)

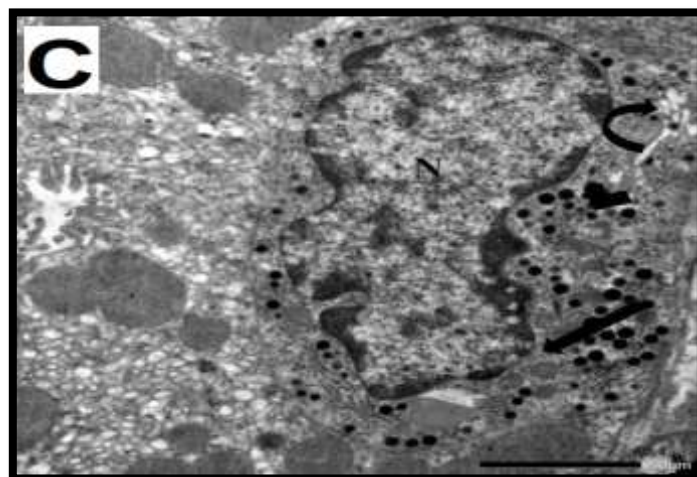
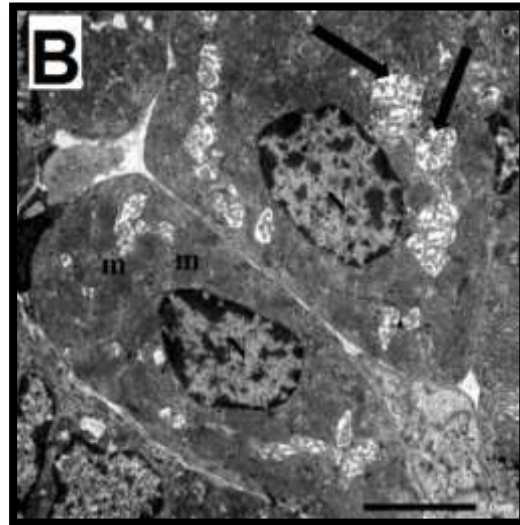
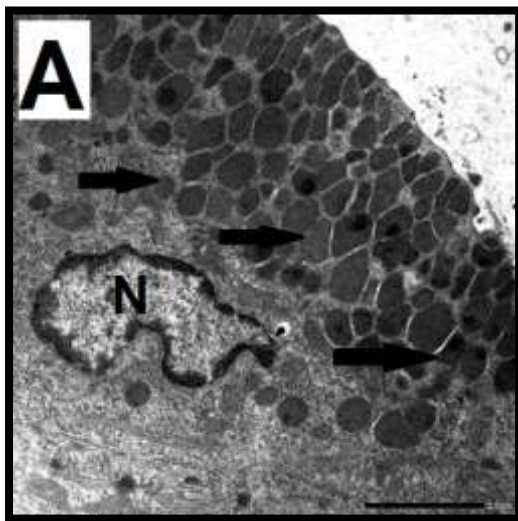


**Fig. (10) (A)** An electron micrograph of surface columnar cell of fundal gastric mucosa from group IV showed indented nucleus (N) surrounded by homogenous cytoplasm, mitochondria, rough endoplasmic reticulum, apical mucinogen granules (arrows). (TEM X7000)

**(B):** An electron micrograph of parietal cell of fundal gastric mucosa from group IV showed, two large pyramidal cells with regular normal spherical nucleus (N) surrounded with large number of normal mitochondria (m). Note, mild damaged in intracellular canaliculi can be seen (arrow). (TEM X 7000)

**(C):** An electron micrograph of enteroendocrine cell of fundal gastric mucosa from group IV showed irregular indented nucleus (N) surrounded by normal RER, homogenous cytoplasm (arrow), secretory granules (arrowhead) and dilated golgi (curved arrow) can be observed. (TEM X 20000)

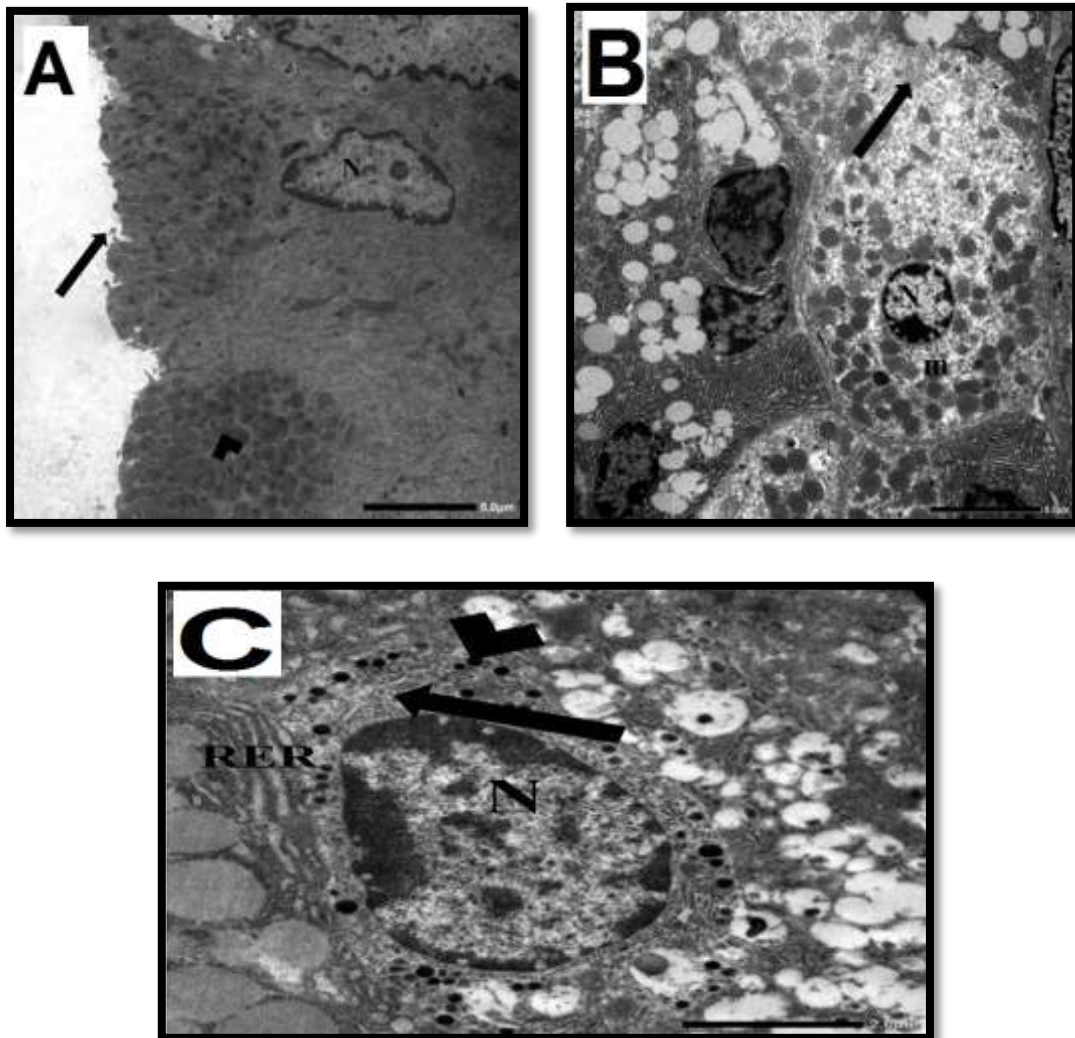


**Fig. (11) (A)** An electron micrograph of surface columnar cell of fundal gastric mucosa from group III appeared tall columnar cell had apical microvilli (arrow), apical mucinogen granules (arrowhead) and basal oval nucleus(N)with prominent nucleolus. (TEM X7000)

**(B):** An electron micrograph of parietal cell of the fundal gastric mucosa from group III showed, regular normal spherical nucleus (N) surrounded with large number of mitochondria (m); intracellular canaliculi (arrow). (TEM X 7000)

**(C):** An electron micrograph of enteroendocrine cell of fundal gastric mucosa from group III showed regular rounded nucleus (N) surrounded by normal RER, homogenous cytoplasm (arrow), secretory granules (arrowhead). (TEM X 20000)

Note mild depletion of secretory granules can be detected

## **DISCUSSION:**

Five-fluorouracil is a potent antimetabolite chemotherapeutic medication. It is commonly implicated in the treatment of various malignancies such as colorectal, liver, breast, head, neck and skin, cancers (Bachmeier et al., 2019).

This research aimed to assess the 5-FU toxic effect of on gastric mucosal and compare between beneficial regenerative effects of BMMSCs and Astaxanthin on 5-FU induced gastric mucosal injury.

In the present study, H&E-stained sections from the rats' stomach fundal mucosa which received 5-FU revealed massive dilated congested blood capillaries, separation in the gastric glands, exfoliation and desquamation of the superficial gastric epithelium and vacuolations of parietal cells with pyknotic nuclei. Also distorted chief cells with pyknotic nuclei and extensive infiltration of mononuclear cells between the fundal glands. There was also a deep ulceration reaching the muscularis mucosa. In the same group, PAS-stained fundal gastric mucosa sections revealed full depletion of the mucous layer.

These finding in agreement with (Kuznietsova and Luzhenetska, 2014), (El-Bermawy, 2015), (Aldo et al., 2016) and (Manar and Dalia 2020) who found that the stomach in the 5-FU exposed rats had a deformed cytoskeleton, increased necrotic cell counts, reduction of villi, atrophy, crypts and muscular layer, associated with edema, disruption of crypts, inflammatory infiltrate and vacuolization.

Also, Kotani et al., (2007) reported that treatment with 5-FU altered the structure and function of gastric mucosa, increasing mucosal susceptibility to acid.

Astaxanthin is a potent anti-cancer and anti-inflammatory antioxidant. Astaxanthin reduces mitochondrial dysfunction and oxidative stress-related diseases and inhibits stomach inflammation via its antioxidant properties. Astaxanthin repairs the rat stomach mucosa by enhancing the activity of free radical-scavenging enzymes such as glutathione peroxidase, catalase, and superoxide dismutase. (Kim et al., 2018).

The present work demonstrated that Astaxanthin had a protective effect against 5-FU-induced gastritis of gastric epithelial cells. This finding in agreement with other animal studies which found that, Astaxanthin reduces thrombosis (Khan, et al, 2020), reduces lipid peroxidation (Iwamoto, et al, 2000), and reduces inflammation (Ohgami et al., 2003).

Also, Nakao et al., (2010) reported that animals which administered 0.08 % Astaxanthin had a greater potential and contractility index of cardiac mitochondrial membrane than control animals. And also demonstrated that astaxanthin decreases inflammation and mitochondrial dysfunction caused by oxidative stress.

Astaxanthin, a potent antioxidant, has been found to stimulate DNA repair in UV-exposed neuroblastoma cells (Santocono et al., 2006). It inhibits DNA damage induced by UVA and stimulates the synthesis of oxidative stress-responsive enzymes (Camera et al., 2008). Astaxanthin significantly reduces the mitochondrial dysfunctions caused by 6-OHDA, such as poly (ADP-ribose) polymerase cleavage, reduced membrane potential, caspase 3 and caspase 9 activation (Ikeda et al., 2008).

Manabe et al., (2008) discovered that Astaxanthin nuclear transcription factor activation and inhibits ROS production induced by hyperglycemia in human mesangial cells. These nuclear transcription factors include transforming growth factor-beta 1 (TGF-1), activation protein-1 (AP-1), nuclear factor kappa B (NFkB), and monocyte chemoattractant protein-1 (MCP-1). AST provides a chemopreventive action due to the significant overexpression of connexin-43 and the strengthening of gap junctional intercellular communication, which supports cellular formation, development, and homeostasis. (Hix et al., 2004).

In the present study, group IV revealed more or less normal apical surface columnar epithelium, mucous neck cells with flat basal nuclei. Parietal cells appeared rounded with central vesicular nuclei & acidophilic cytoplasm, vacuolated cytoplasm was observed in few parietal cells, ki67 immunostained fundal gastric mucosa of group IV showing mild positive Ki67 immunoreaction was observed in little number of proliferative cells lining the isthmus, also sections from of group IV revealing positive PAS stain as bright colour of the mucous cells of the surface epithelium and lining the gastric pits, this mean that the use of MSCs in treatment of harmful effect of 5-FU on the gastric mucosa was very effective.

In the present study, sections from group IV revealed that MSCs transplantation accelerated stomach healing after the injury caused by 5-FU which was inconsistent with Yujiro et al.,(2008) and Chang et al.,(2012) found that stomach healing is significantly accelerated by MSCs transplantation compared to controls and demonstrated that BM-MSCs produced mRNAs for specific angiogenic factors, such as vascular endothelial growth factor (VEGF) and hepatocyte growth factor (HGF). In addition, MSCs injections significantly increased HGF and VEGF gene expression compared to the gastric ulcer group. Human body uses apoptosis to maintain homeostasis throughout development and in response to external stresses (Chi-Chang et al., 2014). The proapoptotic protein interaction involving Bcl-2, which is considered an indicator of anti-apoptotic factors and is receiving increased attention from researchers, and BAX and caspase-3, which are considered indicators of apoptotic cell death, regulate the cytochrome c release, the central gate in activating or inhibiting apoptosis (Chi-Chang et al., 2014) & (Zhang et al., 2012). In line with our findings, (Jacobo et al., 2013) reported that BM-MSCs suppressed apoptosis in stomach mucosal

epitheliocytes and promoted ulcer healing. This is congruent with the findings of (Guangxin et al., 2013).

**Conclusion:** BM-MSCs and Astaxanthin have good effect in ameliorating the toxic effect of 5-FU on the gastric mucosa of albino rats, with no significant difference between the two techniques

**Conflicts of Interest:** The authors declare no conflict of interest.

## References:

**Aldo, C., Ítalo, M., Marília, L., et al. (2018):** Effects of simvastatin on 5-fluorouracil-induced gastrointestinal mucositis in rats. *Rev Col Bras Cir* 45(5):1968-1980.

**Alexandra, K., Tanja, A., Svenja, W., et al. (2017):** Labeling Mesenchymal Stromal Cells with PKH26 or Vybrant Dil Significantly Diminishes their Migration, but does not affect their Viability, Attachment, Proliferation and Differentiation Capacities. *Journal of Tissue Science & Engineering*, 8:2

**Askarov, M., Vostrikova, O., Vorobjova, N., et al. (2008):** Effects of autologous bone marrow cells on apoptosis and regeneration of non-healing autoimmune gastric ulcers. *Bull. Exp. Biol. Med.*, 146: 647–651.

**Bachmeier, E., López, M., Linares, J. et al. (2019):** 5-Fluorouracil and Cyclophosphamide modify functional activity in submandibular gland of rats. *J. Oral Res*, 8: 363–369.

**Bancroft, J., Suvarna, K., Layton, C., (2018):** Bancroft, sTheory and Practice of Histological Techniques, eighth ed.

**Benson, A., Venook, A., Cederquist L., et al (2017):** Colon cancer, version 1.2017, NCCN clinical practice guidelines in oncology. *J Natl Compr Canc Netw*. 15:370–398.

**Bruno, S., Grange, F., Collino, M., et al. (2012):** Microvesicles derived from mesenchymal stem cells enhance survival in a lethal model of acute kidney injury, *PLoS One* 7 (3).

**Camera, E., Matrofrancesco, A., Fabbri, F., et al. (2008):** Astaxanthin, canthaxanthin and beta-carotene differently affect UVA-induced oxidative damage and expression of oxidative stress-responsive enzymes, *Exp. Dermatol.*, in press.

**Chang, Q., Yan, L., Wang, C., et al. (2012):** In vivo transplantation of bone marrow mesenchymal stem cells accelerates repair of injured gastric mucosa in rats. *Chin. Med. J.* 125, 1169–1174 [PMID: 22613549]

**Chi-Chang, H., Yi-Ming, C., Dean-Chuan, W., et al. (2014):** Cytoprotective effect of American ginseng in a rat ethanol gastric ulcer model. *Molecules*, 19, 316–326.

**El-Bermawy, M., (2015):** Light and scanning electron microscopic study of 5-fluorouracil-induced mucosal injury in the gastric fundus and the possible protective role of omeprazole in adult male albino rat. *The Egyptian Journal of Histology.*, 38 (3 ): 415–426.

**Ferlay, J., Soerjomataram, I., Dikshit, R., et al (2015):** Cancer Incidence and Mortality Worldwide: Sources, methods and major patterns in GLOBOCAN 2012. *Int. J. Cancer* 2015, 136, E359–E386.

**Gawish S., Nosseir D., Omar N., et al. (2013):** Histological and Ultra Structural Study of 5-fluorouracil-induced Small Intestinal Mucosal Damage in Rats. *Asian Journal of Cell Biology* 8: 1-21.

**Gorkem A., Huseyin E., Levent T., et al. (2018):** The protective effect of astaxanthin against cisplatin-induced nephrotoxicity in rats. *Biomedicine & Pharmacotherapy* 100 575-582

**Guangxin, J., Gongcai, Q., Dequan, H., et al. (2013):** Allogeneic bone marrow-derived mesenchymal stem cells attenuate hepatic ischemia-reperfusion injury by suppressing oxidative stress and inhibiting apoptosis in rats. *Int. J. Mol. Med.* 31 (6): 1395–1401, 1340.

**Hix, L., Lockwood, J., Bertram, (2004):** Upregulation of connexin 43 protein expression and increased gap junctional communication by water soluble disodium disuccinate astaxanthin derivatives, *Cancer Lett.*, 211 (1): 25–37.

**Ikeda, S., Tsuji, A., Satoh, M., et al. (2008):** Protective effects of astaxanthin on 6-hydroxydopamine-induced apoptosis in human neuroblastoma SH-SY5Y cells, *J. Neurochem.* 107 (6): 1730–1740.

**Iwamoto, T., Hosoda, K., Hirano, R., et al. (2000):** Inhibition of low-density lipoprotein oxidation by astaxanthin. *J. Atheroscler. Thromb.*, 7: 216–222.

**Jacobo, T., Tihomir, G., Mariano, G., et al. (2013):** Regenerative medicine and cell therapy. *Stem Cell Biol. Regener. Med.* 24, 5–277.

**Kataoka Y., Iimori M., Niimi S., et al. (2010):** Cytotoxicity of trifluridine correlates with the thymidine kinase 1 expression level. *Sci Rep.*, 9:79642019.

**Khan, S., Malinski, T., Mason, R., et al. (2010):** Novel astaxanthin prodrug (CDX-085) attenuates thrombosis in a mouse model. *Thromb. Res.* 126: 299–305.

**Kim S., Christopher L., John D., et al (2019):** Theory and practice of histological techniques. 8th ed. China, Churchill Livingstone, Elsevier P. 126 .

**Kim, S., Kim, H. (2018):** Inhibitory effect of astaxanthin on oxidative stress-induced mitochondrial dysfunction-A mini-review. *Nutrients* 10: 1137.

**Kuznietsova N. and Luzhenetska V. (2014):** the state of rat gastric mucosa under the influence of cytostatics: dihydropyrrrol derivative 5-FU and their combination. *Studia Biologica •Tom 8/No1 • C.* 85–92

**Liu, L., Chiu, P., Lam, P., et al. (2015):** Effect of local injection of mesenchymal stem cells on healing of sutured gastric perforation in an experimental model. *Br. J. Surg.*, 102 (2):158–68.

**Manabe, E., Handa, O., Naito Y., et al. (2008):** Astaxanthin protects mesangial cells from hyperglycemia-induced oxidative signaling, *J. Cell Biochem.* 103 (6) : 1925–1937.

**Manar, A., and Dalia, A., (2020) :**Light and Electron Microscopic Studies on the Possible Protective Effect of Ginger on the Gastric Fundic Mucosa of Adult Male

**Mosaad, Y., Abd El Khalik G., Hussein, M., et al. (2016);** a Astaxanthin promising protector against gentamicin-induced nephrotoxicity in rats, *Curr. Pharm. Biotechnol.* 17 (13): 1189–1197.

**Nakao, R., Nelson, O., Park, J., et al. (2010):** Effect of astaxanthin supplementation on inflammation and cardiac function in BALB/c mice. *Anticancer Res.*, 30: 2721–2725.

**Ohgami, K., Shiratori, K., Kotake, S., et al. (2003):** Effects of astaxanthin on lipopolysaccharide-induced inflammation in vitro and in vivo. *Investig. Ophthalmol. Vis. Sci.*, 44, 2694–2701.

**Rashed, L., Gharib, M., Hussein, E., et al. (2016):** Combined effect of bone marrow derived mesenchymal stem cells and nitric oxide inducer on injured gastric mucosa in a rat model. *Tissue and Cell*, 48(6): 644-652.

**Santocono M., Zurria, M., Berrettini, M., et al. (2006):** Influence of astaxanthin, zeaxanthin and lutein on DNA damage and repair in UVA-irradiated cells, *J Photochem. Photobiol. B* 85 (3): 205–215.

**Takkem, A., Barakat, C., Zakaraia, S., et al. (2018):** Ki-67 prognostic value in different histological grades of oral epithelial dysplasia and oral squamous cell carcinoma. *Asian Pacific Journal of Cancer Prevention*, 19(11): 3279– 3286.

**Yujiro, H., Shingo, T., Masahiko, T., et al. (2008):** Sunao Kawano Topical transplantation of mesenchymal stem cells accelerates gastric ulcer healing in rats. *Am. J. Physiol. Gastrointest. Liver Physiol.*, 294, 778–786.

**Zhang, C., Helmsing, S., Zagrebelsky, M., et al. (2012):** Suppression of p75 neurotrophin receptor surface expression with intrabodies influences Bcl-xL mRNA expression and neurite outgrowth in PC12Cells. *PLoS One* 7:30684.

## الملخص العربي

# الخلايا الجذعية الوسيطة المشتقة من نخاع العظام مقابل أستازانثين في علاج التأثير السام الناجم عن عقار ٥- فلورويوراسيل علي الاغشيه المخاطيه لمعدة ذكور الجرذان البيضاء

الخلاصة: يعتبر عقار ٥-فلورويوراسيل دواء فعال في العلاج الكيميائي حيث يشيع استخدامه في علاج الأورام الخبيثة المختلفة. يهدف هذا البحث إلى التحقيق في التأثير العلاجي المحتمل لـ للخلايا الجذعية الوسيطة المشتقة من نخاع العظام وعقار الاستازانثين على التأثير السام الذي يسببه عقار ال٥ فلورويوراسيل على معدة الجرذان البيضاء . تم تقسيم الجرذان الاربعين إلى اربعة مجموعات: المجموعة الأولى (المجموعة الضابطة): لا تتلقى أي علاج المجموعة الثانية (مجموعة ٥- فلورويوراسيل): لمدة ٥ أيام متتالية تم حقنها عن طريق الوريد بمقدار ٥٠ مجم / كجم ٥-فلورو يوراسيل. المجموعة الثالثة (مجموعة ٥-فلورويوراسيل وأستازانثين): حصلت على ٥-فلورو يوراسيل كما في المجموعة الثانية ، يليها أستازانثين ٥٠ مجم / كجم لمدة عشره أيام متتالية. المجموعة الرابعة: مجموعته الخلايا الجذعية الوسيطة: تلقت ٥-فلورو يوراسيل كما في المجموعة الثانية ثم تم حقنها عن طريق الوريد بواسطة  $10^6$  من الخلايا الجذعية الوسيطة مرة واحدة في ذيل الفئران. تم التضحية بجميع الفئران في اليوم الخامس والثلاثين من بداية التجربة ، ليتم فحصها مجهرياً ، وتم صباغه أقسام المعدة بواسطة صبغه الهيماتوكسلين والايوسين ولتقييم إنتاج البروتين السكري المخاطي تم صباغتها بصبغه ال PAS ، المجهر الإلكتروني للإرسال لتقييم التغييرات الهيكلية الفائقة والكيمياء المناعية باستخدام Ki67 تم استخدامها لتقييم مستوى تكاثر الخلايا. أظهر فحص أقسام المعدة من المجموعة الثانية انفصلاً في الغدد المعوية ، واحتقان الشعيرات الدموية ، وتفتحات الخلايا الجدارية ، بينما أظهرت المجموعة الثالثة والرابعة تحسناً ملحوظاً في التركيب النسيجي للمعدة وانخفاضاً منظماً في تعبير Ki67 ، مقارنة بالمجموعه الثانيه و دعم المجهر الإلكتروني هذه النتائج.

وقد اثبتت النتائج أن كل من الخلايا الجذعية الوسيطة و عقار الاستازانثين لهما تأثير جيد في تخفيف التأثير السام لالتهاب المعدة الناجم عن ٥-فلورويوراسيل في الجرذان البيضاء ، مع عدم وجود فرق كبير بين كلتا الطريقتين.



بسم الله الرحمن الرحيم



Mansoura Journal of  
Forensic Medicine  
& Clinical Toxicology

مجلة المنصورة للطب الشرعي  
والسموم الإكلينيكية  
كلية الطب - جامعة المنصورة

### إذن قبول مقالة للنشر بالمجلة

السيد الزميل الدكتور  
أ.م.ع. محمد سعيد الشاذلي  
و زوجه حور هده و نخلاء هاجر هريج  
و أسماء حسن عبد الخالق حسين و ياد من محمد سامعيل السيد  
و هادي محمد نصر و علي محمد علي

تحية طيبة وبعد ..

Bone marrow derived  
mesenchymal stem cells versus Astaxanthin  
in treatment of toxic effect of 5-Fluorouracil  
on gastric mucosa of male albino rats

• الوارد للمجلة بتاريخ ١٦ / ١١ / ٢٠٢٢

مجلة المنصورة  
لطب الشرعي  
والسموم الإكلينيكية

• قد قبل للنشر بالمجلة بتاريخ ١٥ / ١٢ / ٢٠٢٢

وتفضلوا بقبول وافر الاحترام ..

رئيس التحرير  
د. محمد باقر الحنفى